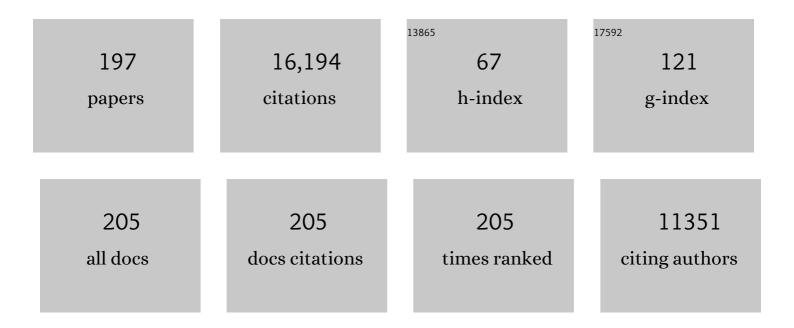
Trevor Douglas

List of Publications by Year in descending order

Source: https://exaly.com/author-pdf/6167473/publications.pdf Version: 2024-02-01



TREVOR DOLICIAS

#	Article	IF	CITATIONS
1	Magnetodendrimers allow endosomal magnetic labeling and in vivo tracking of stem cells. Nature Biotechnology, 2001, 19, 1141-1147.	17.5	1,016
2	Host–guest encapsulation of materials by assembled virus protein cages. Nature, 1998, 393, 152-155.	27.8	887
3	Inorganic-Organic Nanotube Composites from Template Mineralization of Tobacco Mosaic Virus. Advanced Materials, 1999, 11, 253-256.	21.0	698
4	Viruses: Making Friends with Old Foes. Science, 2006, 312, 873-875.	12.6	568
5	Biological Containers: Protein Cages as Multifunctional Nanoplatforms. Advanced Materials, 2007, 19, 1025-1042.	21.0	518
6	Protein Engineering of a Viral Cage for Constrained Nanomaterials Synthesis. Advanced Materials, 2002, 14, 415-418.	21.0	365
7	Targeting of Cancer Cells with Ferrimagnetic Ferritin Cage Nanoparticles. Journal of the American Chemical Society, 2006, 128, 16626-16633.	13.7	359
8	Synthesis and Structure of an Iron(III) Sulfide-Ferritin Bioinorganic Nanocomposite. Science, 1995, 269, 54-57.	12.6	293
9	Nanophase Cobalt Oxyhydroxide Mineral Synthesized within the Protein Cage of Ferritin. Inorganic Chemistry, 2000, 39, 1828-1830.	4.0	278
10	Nanoreactors by Programmed Enzyme Encapsulation Inside the Capsid of the Bacteriophage P22. ACS Nano, 2012, 6, 5000-5009.	14.6	238
11	Classical and quantum magnetic phenomena in natural and artificial ferritin proteins. Science, 1995, 268, 77-80.	12.6	236
12	Plant Viruses as Biotemplates for Materials and Their Use in Nanotechnology. Annual Review of Phytopathology, 2008, 46, 361-384.	7.8	233
13	From The Cover: The structure of a thermophilic archaeal virus shows a double-stranded DNA viral capsid type that spans all domains of life. Proceedings of the National Academy of Sciences of the United States of America, 2004, 101, 7716-7720.	7.1	219
14	Encapsulation of an Enzyme Cascade within the Bacteriophage P22 Virus-Like Particle. ACS Chemical Biology, 2014, 9, 359-365.	3.4	213
15	The ferritin superfamily: Supramolecular templates for materials synthesis. Biochimica Et Biophysica Acta - General Subjects, 2010, 1800, 834-845.	2.4	210
16	Biomimetic Synthesis and Characterization of Magnetic Proteins (Magnetoferritin). Chemistry of Materials, 1998, 10, 279-285.	6.7	204
17	Paramagnetic viral nanoparticles as potential high-relaxivity magnetic resonance contrast agents. Magnetic Resonance in Medicine, 2005, 54, 807-812.	3.0	198
18	Virus Particles as Templates for Materials Synthesis. Advanced Materials, 1999, 11, 679-681.	21.0	189

#	Article	IF	CITATIONS
19	Synthesis and Characterization of Soluble Iron Oxideâ^Dendrimer Composites. Chemistry of Materials, 2001, 13, 2201-2209.	6.7	189
20	Reconstitution of manganese oxide cores in horse spleen and recombinant ferritins. Journal of Inorganic Biochemistry, 1995, 58, 59-68.	3.5	187
21	Protein Cage Constrained Synthesis of Ferrimagnetic Iron Oxide Nanoparticles. Advanced Materials, 2002, 14, 1562-1565.	21.0	184
22	Self-assembling biomolecular catalysts for hydrogen production. Nature Chemistry, 2016, 8, 179-185.	13.6	170
23	The Small Heat Shock Protein Cage from Methanococcus jannaschii Is a Versatile Nanoscale Platform for Genetic and Chemical Modification. Nano Letters, 2003, 3, 1573-1576.	9.1	165
24	Preparation of Magnetically Labeled Cells for Cell Tracking by Magnetic Resonance Imaging. Methods in Enzymology, 2004, 386, 275-299.	1.0	164
25	Use of the interior cavity of the P22 capsid for site-specific initiation of atom-transfer radical polymerization with high-density cargo loading. Nature Chemistry, 2012, 4, 781-788.	13.6	163
26	Magnetoferritin: Characterization of a novel superparamagnetic MR contrast agent. Journal of Magnetic Resonance Imaging, 1994, 4, 497-505.	3.4	162
27	Constrained Synthesis of Cobalt Oxide Nanomaterials in the 12-Subunit Protein Cage fromListeria innocua. Inorganic Chemistry, 2003, 42, 6300-6305.	4.0	152
28	Calculated electrostatic gradients in recombinant human H hain ferritin. Protein Science, 1998, 7, 1083-1091.	7.6	148
29	Genetically Programmed In Vivo Packaging of Protein Cargo and Its Controlled Release from Bacteriophage P22. Angewandte Chemie - International Edition, 2011, 50, 7425-7428.	13.8	147
30	Melanoma and Lymphocyte Cell-Specific Targeting Incorporated into a Heat Shock Protein Cage Architecture. Chemistry and Biology, 2006, 13, 161-170.	6.0	146
31	Protein cage assembly across multiple length scales. Chemical Society Reviews, 2018, 47, 3433-3469.	38.1	138
32	Bio-inspired Synthesis of Protein-Encapsulated CoPt Nanoparticles. Advanced Functional Materials, 2005, 15, 1489-1494.	14.9	136
33	A human ferritin iron oxide nanoâ€composite magnetic resonance contrast agent. Magnetic Resonance in Medicine, 2008, 60, 1073-1081.	3.0	134
34	Comparative Genomic Analysis of Hyperthermophilic Archaeal Fuselloviridae Viruses. Journal of Virology, 2004, 78, 1954-1961.	3.4	131
35	Viral capsids as MRI contrast agents. Magnetic Resonance in Medicine, 2007, 58, 871-879.	3.0	120
36	Biomimetic Synthesis of a H2 Catalyst Using a Protein Cage Architecture. Nano Letters, 2005, 5, 2306-2309.	9.1	119

3

#	Article	IF	CITATIONS
37	From The Cover: An archaeal antioxidant: Characterization of a Dps-like protein from Sulfolobus solfataricus. Proceedings of the National Academy of Sciences of the United States of America, 2005, 102, 10551-10556.	7.1	114
38	Inducible Bronchus-Associated Lymphoid Tissue Elicited by a Protein Cage Nanoparticle Enhances Protection in Mice against Diverse Respiratory Viruses. PLoS ONE, 2009, 4, e7142.	2.5	113
39	Biodistribution studies of protein cage nanoparticles demonstrate broad tissue distribution and rapid clearance in vivo. International Journal of Nanomedicine, 2007, 2, 715-33.	6.7	111
40	2-D Array Formation of Genetically Engineered Viral Cages on Au Surfaces and Imaging by Atomic Force Microscopy. Journal of the American Chemical Society, 2003, 125, 10806-10807.	13.7	106
41	Human ferritin cages for imaging vascular macrophages. Biomaterials, 2011, 32, 1430-1437.	11.4	105
42	Virus-like particle nanoreactors: programmed encapsulation of the thermostable CelB glycosidase inside the P22 capsid. Soft Matter, 2012, 8, 10158.	2.7	100
43	Protein Cage Nanoparticles Bearing the LyP-1 Peptide for Enhanced Imaging of Macrophage-Rich Vascular Lesions. ACS Nano, 2011, 5, 2493-2502.	14.6	98
44	Biomimetic Antigenic Nanoparticles Elicit Controlled Protective Immune Response to Influenza. ACS Nano, 2013, 7, 3036-3044.	14.6	98
45	Targeting and Photodynamic Killing of a Microbial Pathogen Using Protein Cage Architectures Functionalized with a Photosensitizer. Langmuir, 2007, 23, 12280-12286.	3.5	97
46	Heterologous expression of the modified coat protein of Cowpea chlorotic mottle bromovirus results in the assembly of protein cages with altered architectures and function. Journal of General Virology, 2004, 85, 1049-1053.	2.9	96
47	Structural and Functional Studies of Archaeal Viruses. Journal of Biological Chemistry, 2009, 284, 12599-12603.	3.4	96
48	Particle Assembly and Ultrastructural Features Associated with Replication of the Lytic Archaeal Virus <i>Sulfolobus</i> Turreted Icosahedral Virus. Journal of Virology, 2009, 83, 5964-5970.	3.4	96
49	Molecular precursors for indium phosphide and synthesis of small III-V semiconductor clusters in solution. Inorganic Chemistry, 1991, 30, 594-596.	4.0	91
50	Synthetic Control over Magnetic Moment and Exchange Bias in All-Oxide Materials Encapsulated within a Spherical Protein Cage. Journal of the American Chemical Society, 2007, 129, 197-201.	13.7	91
51	Implementation of P22 Viral Capsids as Nanoplatforms. Biomacromolecules, 2010, 11, 2804-2809.	5.4	87
52	Characterization of the Archaeal Thermophile Sulfolobus Turreted Icosahedral Virus Validates an Evolutionary Link among Double-Stranded DNA Viruses from All Domains of Life. Journal of Virology, 2006, 80, 7625-7635.	3.4	86
53	Modular Self-Assembly of Protein Cage Lattices for Multistep Catalysis. ACS Nano, 2018, 12, 942-953.	14.6	86
54	Synthesis and Crystal Structure of a Phospholyl Anion. Angewandte Chemie International Edition in English, 1989, 28, 1367-1368.	4.4	85

#	Article	IF	CITATIONS
55	Photochemical Mineralization of Europium, Titanium, and Iron Oxyhydroxide Nanoparticles in the Ferritin Protein Cage. Inorganic Chemistry, 2008, 47, 2237-2239.	4.0	85
56	Transcriptome Analysis of Infection of the Archaeon <i>Sulfolobus solfataricus</i> with <i>Sulfolobus</i> Turreted Icosahedral Virus. Journal of Virology, 2008, 82, 4874-4883.	3.4	84
57	Biomedical and Catalytic Opportunities of Virus-Like Particles in Nanotechnology. Advances in Virus Research, 2017, 97, 1-60.	2.1	82
58	Iron and Cobalt Oxide and Metallic Nanoparticles Prepared from Ferritin. Langmuir, 2004, 20, 10283-10287.	3.5	80
59	Photocatalytic Synthesis of Copper Colloids from Cu(II) by the Ferrihydrite Core of Ferritin. Inorganic Chemistry, 2004, 43, 3441-3446.	4.0	79
60	Synthesis of a Cross-Linked Branched Polymer Network in the Interior of a Protein Cage. Journal of the American Chemical Society, 2009, 131, 4346-4354.	13.7	77
61	MATERIALS SCIENCE: A Bright Bio-Inspired Future. Science, 2003, 299, 1192-1193.	12.6	76
62	Biomimetic synthesis of \hat{I}^2 -TiO2 inside a viral capsid. Journal of Materials Chemistry, 2008, 18, 3821.	6.7	75
63	Programmed Self-Assembly of an Active P22-Cas9 Nanocarrier System. Molecular Pharmaceutics, 2016, 13, 1191-1196.	4.6	73
64	A radical solution for the biosynthesis of the H-cluster of hydrogenase. FEBS Letters, 2006, 580, 363-367.	2.8	72
65	Coconfinement of Fluorescent Proteins: Spatially Enforced Communication of GFP and mCherry Encapsulated within the P22 Capsid. Biomacromolecules, 2012, 13, 3902-3907.	5.4	71
66	Virus movement maintains local virus population diversity. Proceedings of the National Academy of Sciences of the United States of America, 2007, 104, 19102-19107.	7.1	70
67	Something Old, Something New, Something Borrowed; How the Thermoacidophilic Archaeon Sulfolobus solfataricus Responds to Oxidative Stress. PLoS ONE, 2009, 4, e6964.	2.5	70
68	Controlled Assembly of Bifunctional Chimeric Protein Cages and Composition Analysis Using Noncovalent Mass Spectrometry. Journal of the American Chemical Society, 2008, 130, 16527-16529.	13.7	69
69	P22 Viral Capsids as Nanocomposite High-Relaxivity MRI Contrast Agents. Molecular Pharmaceutics, 2013, 10, 11-17.	4.6	69
70	Design of a VLP-nanovehicle for CYP450 enzymatic activity delivery. Journal of Nanobiotechnology, 2015, 13, 66.	9.1	67
71	Assembly of Multilayer Films Incorporating a Viral Protein Cage Architecture. Langmuir, 2006, 22, 8891-8896.	3.5	66
72	Symmetry Controlled, Genetic Presentation of Bioactive Proteins on the P22 Virus-like Particle Using an External Decoration Protein. ACS Nano, 2015, 9, 9134-9147.	14.6	66

#	Article	IF	CITATIONS
73	Development of virusâ€like particles for diagnostic and prophylactic biomedical applications. Wiley Interdisciplinary Reviews: Nanomedicine and Nanobiotechnology, 2015, 7, 722-735.	6.1	65
74	RGD-Conjugated Human Ferritin Nanoparticles for Imaging Vascular Inflammation and Angiogenesis in Experimental Carotid and Aortic Disease. Molecular Imaging and Biology, 2012, 14, 315-324.	2.6	64
75	A Streptavidina^`Protein Cage Janus Particle for Polarized Targeting and Modular Functionalization. Journal of the American Chemical Society, 2009, 131, 9164-9165.	13.7	63
76	Structure of the DPS-Like Protein fromSulfolobus solfataricusReveals a Bacterioferritin-Like Dimetal Binding Site within a DPS-Like Dodecameric Assemblyâ€,‡. Biochemistry, 2006, 45, 10815-10827.	2.5	61
77	Cargo–shell and cargo–cargo couplings govern the mechanics of artificially loaded virus-derived cages. Nanoscale, 2016, 8, 9328-9336.	5.6	60
78	Photochemical Reactivity of Ferritin for Cr(VI) Reduction. Chemistry of Materials, 2002, 14, 4874-4879.	6.7	59
79	Hot crenarchaeal viruses reveal deep evolutionary connections. Nature Reviews Microbiology, 2006, 4, 520-528.	28.6	59
80	Supramolecular Protein Cage Composite MR Contrast Agents with Extremely Efficient Relaxivity Properties. Nano Letters, 2009, 9, 4520-4526.	9.1	59
81	High-Density Targeting of a Viral Multifunctional Nanoplatform to a Pathogenic, Biofilm-Forming Bacterium. Chemistry and Biology, 2007, 14, 387-398.	6.0	58
82	Synergistic Effects of Mutations and Nanoparticle Templating in the Self-Assembly of Cowpea Chlorotic Mottle Virus Capsids. Nano Letters, 2009, 9, 393-398.	9.1	57
83	Tailored delivery of analgesic ziconotide across a blood brain barrier model using viral nanocontainers. Scientific Reports, 2015, 5, 12497.	3.3	56
84	Structural transitions in Cowpea chlorotic mottle virus (CCMV). Physical Biology, 2005, 2, S166-S172.	1.8	54
85	Modular interior loading and exterior decoration of a virus-like particle. Nanoscale, 2017, 9, 10420-10430.	5.6	54
86	Synthesis and characterization of hydrophobic ferritin proteins. Journal of Inorganic Biochemistry, 1999, 76, 187-195.	3.5	52
87	Metal binding to cowpea chlorotic mottle virus using terbium(III) fluorescence. Journal of Biological Inorganic Chemistry, 2003, 8, 721-725.	2.6	52
88	Templated Assembly of a Functional Ordered Protein Macromolecular Framework from P22 Virus-like Particles. ACS Nano, 2018, 12, 3541-3550.	14.6	52
89	Viruslike Particles Encapsidating Respiratory Syncytial Virus M and M2 Proteins Induce Robust T Cell Responses. ACS Biomaterials Science and Engineering, 2016, 2, 2324-2332.	5.2	50
90	Dps-like protein from the hyperthermophilic archaeon Pyrococcus furiosus. Journal of Inorganic Biochemistry, 2006, 100, 1061-1068.	3.5	49

#	Article	IF	CITATIONS
91	Intracellular Distribution of Macrophage Targeting Ferritin–Iron Oxide Nanocomposite. Advanced Materials, 2009, 21, 458-462.	21.0	48
92	Correlative Lightâ€Electron Microscopy Shows RGDâ€Targeted ZnO Nanoparticles Dissolve in the Intracellular Environment of Triple Negative Breast Cancer Cells and Cause Apoptosis with Intratumor Heterogeneity. Advanced Healthcare Materials, 2016, 5, 1310-1325.	7.6	48
93	Influence of Electrostatic Interactions on the Surface Adsorption of a Viral Protein Cage. Langmuir, 2005, 21, 8686-8693.	3.5	47
94	Janus-like Protein Cages. Spatially Controlled Dual-Functional Surface Modifications of Protein Cages. Nano Letters, 2009, 9, 2360-2366.	9.1	47
95	Surface contribution to the anisotropy energy of spherical magnetite particles. Journal of Applied Physics, 2005, 97, 10B301.	2.5	44
96	Templated assembly of organic–inorganic materials using the core shell structure of the P22 bacteriophage. Chemical Communications, 2011, 47, 6326.	4.1	44
97	Ordered association of tobacco mosaic virus in the presence of divalent metal ions. Journal of Inorganic Biochemistry, 2001, 84, 233-240.	3.5	42
98	Classical and quantum magnetism in synthetic ferritin proteins. Journal of Applied Physics, 1996, 79, 5324.	2.5	41
99	Rescuing recombinant proteins by sequestration into the P22 VLP. Chemical Communications, 2013, 49, 10412-10414.	4.1	41
100	Location of the Bacteriophage P22 Coat Protein C-Terminus Provides Opportunities for the Design of Capsid-Based Materials. Biomacromolecules, 2013, 14, 2989-2995.	5.4	41
101	Magnetoferritin. Investigative Radiology, 1994, 29, S214-S216.	6.2	40
102	Monitoring Biomimetic Platinum Nanocluster Formation Using Mass Spectrometry and Clusterâ€Đependent H ₂ Production. Angewandte Chemie - International Edition, 2008, 47, 7845-7848.	13.8	40
103	A click chemistry based coordination polymer inside small heat shock protein. Chemical Communications, 2010, 46, 264-266.	4.1	40
104	RGD targeting of human ferritin iron oxide nanoparticles enhances in vivo MRI of vascular inflammation and angiogenesis in experimental carotid disease and abdominal aortic aneurysm. Journal of Magnetic Resonance Imaging, 2017, 45, 1144-1153.	3.4	40
105	Synthetic Virus-like Particles for Glutathione Biosynthesis. ACS Synthetic Biology, 2020, 9, 3298-3310.	3.8	40
106	Site-Directed Coordination Chemistry with P22 Virus-like Particles. Langmuir, 2012, 28, 1998-2006.	3.5	38
107	Photo-induced H2 production by [NiFe]-hydrogenase from T. roseopersicina covalently linked to a Ru(II) photosensitizer. Journal of Inorganic Biochemistry, 2012, 106, 151-155.	3.5	38
108	A Self-Adjuvanted, Modular, Antigenic VLP for Rapid Response to Influenza Virus Variability. ACS Applied Materials & Interfaces, 2020, 12, 18211-18224.	8.0	38

#	Article	IF	CITATIONS
109	Size and Crystallinity in Protein-Templated Inorganic Nanoparticles. Chemistry of Materials, 2010, 22, 4612-4618.	6.7	37
110	Tuning the catalytic properties of P22 nanoreactors through compositional control. Nanoscale, 2020, 12, 336-346.	5.6	37
111	Constructing catalytic antimicrobial nanoparticles by encapsulation of hydrogen peroxide producing enzyme inside the P22 VLP. Journal of Materials Chemistry B, 2014, 2, 5948.	5.8	36
112	Higher Order Assembly of Virusâ€like Particles (VLPs) Mediated by Multiâ€valent Protein Linkers. Small, 2015, 11, 1562-1570.	10.0	36
113	Interligand Electron Transfer in Heteroleptic Ruthenium(II) Complexes Occurs on Multiple Time Scales. Journal of Physical Chemistry A, 2015, 119, 4813-4824.	2.5	36
114	Initial assessment of magnetoferritin biokinetics and proton relaxation enhancement in rats. Academic Radiology, 1995, 2, 871-878.	2.5	35
115	Sortase-Mediated Ligation as a Modular Approach for the Covalent Attachment of Proteins to the Exterior of the Bacteriophage P22 Virus-like Particle. Bioconjugate Chemistry, 2017, 28, 2114-2124.	3.6	35
116	Tuning Viral Capsid Nanoparticle Stability with Symmetrical Morphogenesis. ACS Nano, 2016, 10, 8465-8473.	14.6	34
117	Expanding the Temperature Range of Biomimetic Synthesis Using a Ferritin from the Hyperthermophile <i>Pyrococcus furiosus</i> . Chemistry of Materials, 2008, 20, 1541-1547.	6.7	32
118	Further Characterisation of Forms of Haemosiderin in Iron-Overloaded Tissues. FEBS Journal, 1994, 225, 187-194.	0.2	31
119	Some Enzymes Just Need a Space of Their Own. Science, 2010, 327, 42-43.	12.6	31
120	A virus-like particle vaccine platform elicits heightened and hastened local lung mucosal antibody production after a single dose. Vaccine, 2012, 30, 3653-3665.	3.8	31
121	Induction of Antiviral Immune Response through Recognition of the Repeating Subunit Pattern of Viral Capsids Is Toll-Like Receptor 2 Dependent. MBio, 2017, 8, .	4.1	31
122	Targeted Delivery of a Photosensitizer to <i>Aggregatibacter actinomycetemcomitans</i> Biofilm. Antimicrobial Agents and Chemotherapy, 2010, 54, 2489-2496.	3.2	30
123	Cargo Retention inside P22 Virus-Like Particles. Biomacromolecules, 2018, 19, 3738-3746.	5.4	30
124	Modeling of the magnetic behavior of γ-Fe2O3 nanoparticles mineralized in ferritin. Journal of Applied Physics, 2004, 95, 7127-7129.	2.5	29
125	Determination of anisotropy constants of protein encapsulated iron oxide nanoparticles by electron magnetic resonance. Journal of Magnetism and Magnetic Materials, 2009, 321, 175-180.	2.3	29
126	Stabilizing viral nano-reactors for nerve-agent degradation. Biomaterials Science, 2013, 1, 881.	5.4	29

#	Article	IF	CITATIONS
127	Molecular exclusion limits for diffusion across a porous capsid. Nature Communications, 2021, 12, 2903.	12.8	29
128	The archaeal Dps nanocage targets kidney proximal tubules via glomerular filtration. Journal of Clinical Investigation, 2019, 129, 3941-3951.	8.2	29
129	Virus-Like Particle-Induced Protection Against MRSA Pneumonia Is Dependent on IL-13 and Enhancement of Phagocyte Function. American Journal of Pathology, 2012, 181, 196-210.	3.8	28
130	Protein cage nanoparticles as secondary building units for the synthesis of 3-dimensional coordination polymers. Soft Matter, 2010, 6, 3167.	2.7	27
131	Structure and photoelectrochemistry of a virus capsid–TiO2nanocomposite. Nanoscale, 2011, 3, 1004-1007.	5.6	27
132	Proteomic Analysis of <i>Sulfolobus solfataricus</i> during <i>Sulfolobus</i> Turreted Icosahedral Virus Infection. Journal of Proteome Research, 2012, 11, 1420-1432.	3.7	26
133	Inducible Bronchus-Associated Lymphoid Tissue (iBALT) Synergizes with Local Lymph Nodes during Antiviral CD4 ⁺ T Cell Responses. Lymphatic Research and Biology, 2013, 11, 196-202.	1.1	26
134	Selective Biotemplated Synthesis of TiO ₂ Inside a Protein Cage. Biomacromolecules, 2015, 16, 214-218.	5.4	26
135	Virus-Like Particles (VLPs) as a Platform for Hierarchical Compartmentalization. Biomacromolecules, 2020, 21, 2060-2072.	5.4	26
136	Atomic force microscopy of virus shells. Biochemical Society Transactions, 2017, 45, 499-511.	3.4	25
137	Virus capsid assembly across different length scales inspire the development of virus-based biomaterials. Current Opinion in Virology, 2019, 36, 38-46.	5.4	25
138	Biomimetic FePt nanoparticle synthesis within Pyrococcus furiosus ferritins and their layer-by-layer formation. Soft Matter, 2011, 7, 11078.	2.7	24
139	Correct charge state assignment of native electrospray spectra of protein complexes. Journal of the American Society for Mass Spectrometry, 2009, 20, 435-442.	2.8	23
140	Atom transfer radical polymerization on the interior of the P22 capsid and incorporation of photocatalytic monomer crosslinks. European Polymer Journal, 2013, 49, 2976-2985.	5.4	23
141	Effects of Culturing on the Population Structure of a Hyperthermophilic Virus. Microbial Ecology, 2004, 48, 561-566.	2.8	22
142	Manganese(III) porphyrins complexed with P22 virus-like particles as T 1-enhanced contrast agents for magnetic resonance imaging. Journal of Biological Inorganic Chemistry, 2014, 19, 237-246.	2.6	22
143	Immobilization of Active Hydrogenases by Encapsulation in Polymeric Porous Gels. Nano Letters, 2005, 5, 2085-2087.	9.1	21
144	Biomimetic synthesis of photoactive α-Fe ₂ O ₃ templated by the hyperthermophilic ferritin from Pyrococus furiosus. Journal of Materials Chemistry, 2010, 20, 65-67.	6.7	21

#	Article	IF	CITATIONS
145	Co-localization of catalysts within a protein cage leads to efficient photochemical NADH and/or hydrogen production. Journal of Materials Chemistry B, 2016, 4, 5375-5384.	5.8	21
146	Linker-Mediated Assembly of Virus-Like Particles into Ordered Arrays via Electrostatic Control. ACS Applied Bio Materials, 2019, 2, 2192-2201.	4.6	21
147	Bioinspired Approaches to Self-Assembly of Virus-like Particles: From Molecules to Materials. Accounts of Chemical Research, 2022, 55, 1349-1359.	15.6	21
148	Mössbauer spectroscopic and magnetic studies of magnetoferritin. Hyperfine Interactions, 1994, 91, 847-851.	0.5	20
149	Characterization of the Bacteroides fragilis bfr Gene Product Identifies a Bacterial DPS-Like Protein and Suggests Evolutionary Links in the Ferritin Superfamily. Journal of Bacteriology, 2012, 194, 15-27.	2.2	20
150	Gadolinium-Loaded Viral Capsids as Magnetic Resonance Imaging Contrast Agents. Applied Magnetic Resonance, 2015, 46, 349-355.	1.2	20
151	Developing a Dissociative Nanocontainer for Peptide Drug Delivery. International Journal of Environmental Research and Public Health, 2015, 12, 12543-12555.	2.6	19
152	Hybrid Nanoreactors: Coupling Enzymes and Smallâ€Molecule Catalysts within Virus‣ike Particles. Israel Journal of Chemistry, 2015, 55, 96-101.	2.3	19
153	Protein nanocage architectures for the delivery of therapeutic proteins. Current Opinion in Colloid and Interface Science, 2021, 51, 101395.	7.4	19
154	Substrate Partitioning into Protein Macromolecular Frameworks for Enhanced Catalytic Turnover. ACS Nano, 2021, 15, 15687-15699.	14.6	19
155	Electron magnetic resonance of iron oxide nanoparticles mineralized in protein cages. Journal of Applied Physics, 2005, 97, 10M523.	2.5	17
156	Stimuli Responsive Hierarchical Assembly of P22 Virus-like Particles. Chemistry of Materials, 2018, 30, 2262-2273.	6.7	17
157	Oriented nucleation of gypsum (CaSO4·2H2O) under compressed Langmuir monolayers. Materials Science and Engineering C, 1994, 1, 193-199.	7.3	16
158	Microbe Manufacturers of Semiconductors. Chemistry and Biology, 2004, 11, 1478-1480.	6.0	16
159	Topological Biosignatures: Large-Scale Structure of Chemical Networks from Biology and Astrochemistry. Astrobiology, 2012, 12, 29-39.	3.0	15
160	A phospholyl complex of indium. Polyhedron, 1990, 9, 329-333.	2.2	14
161	Genetics, biochemistry and structure of the archaeal virus STIV. Biochemical Society Transactions, 2009, 37, 114-117.	3.4	14
162	Changes in the stability and biomechanics of P22 bacteriophage capsid during maturation. Biochimica Et Biophysica Acta - General Subjects, 2018, 1862, 1492-1504.	2.4	14

#	Article	IF	CITATIONS
163	Polymer Coatings on Virus-like Particle Nanoreactors at Low Ionic Strength—Charge Reversal and Substrate Access. Biomacromolecules, 2021, 22, 2107-2118.	5.4	14
164	Two-component magnetic structure of iron oxide nanoparticles mineralized in <i>Listeria innocua</i> protein cages. Journal of Applied Physics, 2010, 107, .	2.5	13
165	Two-Dimensional Crystallization of P22 Virus-Like Particles. Journal of Physical Chemistry B, 2016, 120, 5938-5944.	2.6	13
166	Chemically Induced Morphogenesis of P22 Virus-like Particles by the Surfactant Sodium Dodecyl Sulfate. Biomacromolecules, 2019, 20, 389-400.	5.4	13
167	Use of Protein Cages as a Template for Confined Synthesis of Inorganic and Organic Nanoparticles. Methods in Molecular Biology, 2015, 1252, 17-25.	0.9	13
168	Virus particles as active nanomaterials that can rapidly change their viscoelastic properties in response to dilute solutions. Soft Matter, 2010, 6, 5286.	2.7	12
169	Bioprospecting in high temperature environments; application of thermostable protein cages. Soft Matter, 2007, 3, 1091.	2.7	11
170	Monitoring Structural Transitions in Icosahedral Virus Protein Cages by Site-Directed Spin Labeling. Journal of the American Chemical Society, 2011, 133, 4156-4159.	13.7	11
171	CD11c + cells primed with unrelated antigens facilitate an accelerated immune response to influenza virus in mice. European Journal of Immunology, 2014, 44, 397-408.	2.9	11
172	Signal ampflication using nanoplatform cluster formation. Soft Matter, 2008, 4, 2519.	2.7	10
173	Controlled Modular Multivalent Presentation of the CD40 Ligand on P22 Virus-like Particles Leads to Tunable Amplification of CD40 Signaling. ACS Applied Bio Materials, 2021, 4, 8205-8214.	4.6	10
174	Hydrogen Enhances Nickel Tolerance in the Purple Sulfur Bacterium Thiocapsa roseopersicina. Environmental Science & Technology, 2010, 44, 834-840.	10.0	9
175	Loading the dice: The orientation of virus-like particles adsorbed on titanate assisted organosilanized surfaces. Biointerphases, 2019, 14, 011001.	1.6	9
176	Cytochrome <i>C</i> with peroxidase-like activity encapsulated inside the small DPS protein nanocage. Journal of Materials Chemistry B, 2021, 9, 3168-3179.	5.8	9
177	Persistent oral contrast agent lining the intestine in severe mucosal disease: elucidation of radiographic appearance Radiology, 1994, 191, 747-749.	7.3	8
178	A NETWORK-THEORETICAL APPROACH TO UNDERSTANDING INTERSTELLAR CHEMISTRY. Astrophysical Journal, 2010, 722, 1921-1931.	4.5	8
179	X-ray spatial frequency heterodyne imaging of protein-based nanobubble contrast agents. Optics Express, 2014, 22, 23290.	3.4	8
180	Virus Matryoshka: A Bacteriophage Particle—Guided Molecular Assembly Approach to a Monodisperse Model of the Immature Human Immunodeficiency Virus. Small, 2016, 12, 5862-5872.	10.0	8

#	Article	IF	CITATIONS
181	In Vivo Packaging of Protein Cargo Inside of Virus-Like Particle P22. Methods in Molecular Biology, 2018, 1776, 295-302.	0.9	8
182	Multilayered Ordered Protein Arrays Self-Assembled from a Mixed Population of Virus-like Particles. ACS Nano, 2022, 16, 7662-7673.	14.6	8
183	Electromechanical Photophysics of GFP Packed Inside Viral Protein Cages Probed by Forceâ€Fluorescence Hybrid Singleâ€Molecule Microscopy. Small, 2022, 18, .	10.0	7
184	Ion Accumulation in a Protein Nanocage: Finding Noisy Temporal Sequences Using a Genetic Algorithm. Biophysical Journal, 2010, 99, 3385-3393.	0.5	6
185	All in the Packaging: Structural and Electronic Effects of Nanoconfinement on Metal Oxide Nanoparticles. Chemistry of Materials, 2011, 23, 3921-3929.	6.7	6
186	Inorganic–Organic Nanotube Composites from Template Mineralization of Tobacco Mosaic Virus. Advanced Materials, 1999, 11, 253-256.	21.0	6
187	Structure, dynamics, and solvation in a disordered metal–organic coordination polymer: a multiscale study. Journal of Coordination Chemistry, 2011, 64, 4301-4317.	2.2	5
188	Unravelling capsid transformations. Nature Chemistry, 2013, 5, 444-445.	13.6	5
189	Fluctuating nonlinear spring theory: Strength, deformability, and toughness of biological nanoparticles from theoretical reconstruction of force-deformation spectra. Acta Biomaterialia, 2021, 122, 263-277.	8.3	5
190	In-Plane Ordering of a Genetically Engineered Viral Protein Cage. Journal of Adhesion, 2009, 85, 69-77.	3.0	4
191	Swelling and Softening of the CCMV Plant Virus Capsid in Response toÂpH Shifts. Biophysical Journal, 2010, 98, 656a.	0.5	4
192	Inorganic–Organic Nanotube Composites from Template Mineralization of Tobacco Mosaic Virus. , 1999, 11, 253.		3
193	Charge Development on Ferritin: An Electrokinetic Study of a Protein Containing a Ferrihydrite Nanoparticle. ACS Symposium Series, 2004, , 226-229.	0.5	2
194	Targeted Cancer Therapy: Correlative Lightâ€Electron Microscopy Shows RGDâ€Targeted ZnO Nanoparticles Dissolve in the Intracellular Environment of Triple Negative Breast Cancer Cells and Cause Apoptosis with Intratumor Heterogeneity (Adv. Healthcare Mater. 11/2016). Advanced Healthcare Materials, 2016, 5, 1248-1248.	7.6	2
195	Biomimetic Synthesis of an Active H2 Catalyst Using the Ferritin Protein Cage Architecture. ACS Symposium Series, 2008, , 263-272.	0.5	1
196	A Bioengineering Approach to the Production of Metal and Metal Oxide Nanoparticles. ACS Symposium Series, 2004, , 230-237.	0.5	0
197	Nano-Particulate Platforms for Vaccine Delivery to Enhance Antigen-Specific CD8+ T-Cell Response. Methods in Molecular Biology, 2022, 2412, 367-398.	0.9	0